Hepatocyte-specific deletion of peroxisomal protein PEX13 results in disrupted iron homeostasis

Gautam Rishi[1*], Maneet Bhatia[1*], Eriza S. Secondes[1], Michelle Melino[1], Denis I. Crane[2], V. Nathan Subramaniam[1]

[1]Hepatogenomics Research Group, School of Biomedical Sciences, Institute of Health and Biomedical Innovation, Queensland University of Technology (QUT), Brisbane, Australia. [2]School of Environment and Science, Griffith University, Brisbane, Australia.

*Joint first authors

Short Title: Peroxisomes and iron homeostasis

Gautam Rishi: gautam.rishi@qut.edu.au

Maneet Bhatia: maneet.bhatia@qut.edu.au

Eriza S. Secondes: e.secondes@qut.edu.au

Michelle Melino: michelle.melino83@gmail.com

Denis I. Crane: d.crane@griffith.edu.au

V. Nathan Subramaniam: nathan.subramaniam@qut.edu.au

Corresponding author:

Professor V. Nathan Subramaniam
Institute of Health and Biomedical Innovation and School of Biomedical Sciences, Queensland University of Technology
60 Musk Avenue, Kelvin Grove
Brisbane, QLD 4059, Australia
Tel: ++ 617 313892980
E-mail: nathan.subramaniam@qut.edu.au

Abstract

Peroxisomes are organelles, abundant in the liver, involved in a variety of cellular functions, including fatty acid metabolism, plasmalogen synthesis and metabolism of reactive oxygen species. Several inherited disorders are associated with peroxisomal dysfunction; increasingly many are associated with hepatic pathologies. The liver plays a principal role in regulation of iron metabolism. In this study we examined the possibility of a relationship between iron homeostasis and peroxisomal integrity.

We examined the effect of deleting *Pex13* in mouse liver on systemic iron homeostasis. We also used siRNA-mediated knock-down of *PEX13* in a human hepatoma cell line (HepG2/C3A) to elucidate the mechanisms of PEX13-mediated regulation of hepcidin.

We demonstrate that transgenic mice lacking hepatocyte *Pex13* have defects in systemic iron homeostasis. The ablation of *Pex13* expression in hepatocytes leads to a significant reduction in hepatic hepcidin levels. Our results also demonstrate that a deficiency of *PEX13* gene expression in HepG2/C3A cells leads to decreased hepcidin expression, which is mediated through an increase in the signalling protein *SMAD7*, and endoplasmic reticulum (ER) stress.

This study identifies a novel role for a protein involved in maintaining peroxisomal integrity and function in iron homeostasis. Loss of Pex13, a protein important for peroxisomal function, in hepatocytes leads to a significant increase in ER stress, which if unresolved, can affect liver function. The results from this study have implications for the management of patients with peroxisomal disorders and the liver-related complications they may develop.

Keywords:

Iron metabolism, hemochromatosis, peroxisomal disorders, genetic modifiers, iron overload

Abbreviations:

GNPAT: glyceronephosphate O-acyltransferase

PEX13: peroxin 13

ER: endoplasmic reticulum

SMAD: sma and mothers against decapentaplegic

HFE: the homeostatic iron regulator

HH: hereditary hemochromatosis

BMP: bone morphogenetic protein

TFR2: transferrin receptor 2

HJV: hemojuvelin

PTS: peroxisomal targeting sequences

PED: peroxisomal enzyme disorder

PBD: peroxisomal biogenesis disorder

RCDP: rhizomelic chondrodysplasia punctate

HIC: hepatic iron concentration

SIC: splenic iron concentration

DIC: duodenal iron concentration

CIC: cardiac iron concentration

HPRT: hypoxanthine-guanine phosphoribosyl transferase

RPL13: ribosomal protein L13

POLR2A: DNA directed RNA polymerase II subunit RPB1

UPR: unfolded protein response

Funding Information

This work was supported in part by Project Grants (APP1082224 and APP1100088) from the National Health and Medical Research Council (NHMRC) of Australia to VNS. VNS is the recipient of an NHMRC Senior Research Fellowship (APP1118888).

Disclosure of Conflicts of Interest

The authors declare no conflicts of interest.

Authorship Contributions

GR, MB and VNS designed the study; GR, MB, ESS and MM performed the experiments; GR, MB, ESS, MM, DIC and VNS analyzed the data; DIC provided the *Pex13* floxed mice and Pex13 antibody; GR, MB and VNS wrote the manuscript; all authors critically reviewed the manuscript.

1. Introduction

Peroxisomes are involved in several metabolic functions, including α- and β-oxidation of fatty acids, scavenging of hydrogen peroxide (H_2O_2) generated during this process, and synthesis of ether lipids, such as plasmalogens [1]. Proteins involved in peroxisomal biogenesis are collectively called ‘peroxins’ or ‘PEX’, and play a role in proliferation of peroxisomes, formation of the peroxisomal membrane and import of peroxisomal matrix proteins [2]. In mammalian cells, the peroxisomal import machinery utilizes PEX5 and PEX7 as shuttle proteins which recognize the ‘peroxisomal targeting sequences’ (PTS1 and PTS2 respectively) in cargo proteins and guide them to peroxisomal membranes [3]. The cargo-laden PEX5 and PEX7 then form a transient docking complex with PEX13 and PEX14 proteins, after which the complex is disintegrated to release the cargo, while PEX5 and PEX7 are recycled back into the cytosol [4, 5].

Defects in a number of genes can cause peroxisomal disorders, which are grouped as either single enzyme deficiencies (peroxisomal enzyme disorders or PEDs) or peroxisomal biogenesis disorders (PBDs) [6]. PEDs are caused by the mutation of a single peroxisomal protein and include the disease group called rhizomelic chondrodysplasia punctata (RCDP), specifically RCDP2, 3 and 4. PBDs are caused by mutations in PEX genes, which are required for peroxisome biogenesis or peroxisome proliferation, and characterized by a generalized peroxisomal dysfunction. PBDs include RCDP1 and RCDP5, caused by a defect in PEX7 and PEX5 respectively [7, 8] and the Zellweger syndrome spectrum disorders, caused by defects in the remaining PEX genes, such as PEX5, PEX13 and PEX14 [9, 10]. Some severe PBD cases present with cranial abnormalities, hepatic dysfunction, visual and/or hearing loss, seizures and neural dysfunction [9]. The peroxisomes in the hepatocytes are

required for several essential metabolic functions including β-oxidation. These functions are hampered in the presence of peroxisomal deficiencies and lead to changes in metabolic pathways and ultimately liver dysfunction [11]. There is also some clinical evidence suggesting a dysregulation in iron homeostasis in patients with Zellweger syndrome [12, 13], however, iron metabolism has not been studied in these patients.

Iron is vital for many biological functions; an imbalance in iron levels can result in iron deficiency or iron overloading. A cysteine to tyrosine mutation at position 282 (p.C282Y) in the hemochromatosis protein HFE (the homeostatic iron regulator) is the most common of the genetic iron overload disorder, hereditary hemochromatosis (HH) [14]. As a result of this mutation, patients have low levels of hepcidin (*HAMP*), a liver-expressed peptide, which is the master regulator of iron homeostasis, leading to increased absorption of iron. Hepcidin is primarily activated in response to body iron levels via the bone morphogenetic (BMP)/sma and mothers against decapentaplegic (SMAD) pathway [15].

In the current study, we examined the relationship between peroxisomes and iron homeostasis. To address this, we generated a hepatocyte-specific *Pex13* knock-out mouse model and used siRNA-mediated knock-down of *PEX13* in human hepatoma HepG2/C3A cells. We used these models to study the effect of peroxisomal defects on the expression of hepcidin and its regulation by the BMP-SMAD pathway.

2. Materials and Methods

2.1 Generation of hepatocyte-specific Pex13 knock-out mice

Mice were housed under a 12:12h light/dark cycle and were provided with food and water ad libitum. *Pex13*$^{f/f}$ mice on a C57BL/6J background have been previously described [16]. The homozygous floxed mice were bred with heterozygous *Alb-Cre* [17] mice (also on a C57BL/6J background) to generate the *Pex13* hepatocyte-specific knock-out (*Pex13*$^{f/f}$*/Alb-Cre*$^{+/-}$) and littermate control (*Pex13*$^{f/f}$*/Alb-Cre*$^{-/-}$) mice. For this study, we analyzed female mice at 5 weeks of age. The mice were fasted for 6h before being sacrificed and their tissues collected, which were immediately frozen on dry ice until further use. All animal studies were approved by the University of Queensland and Queensland University of Technology Animal Ethics Committees. Animals received ethical, humane and responsible care according to the criteria outlined in the "*Australian code for the care and use of animals for scientific purposes*, 2013".

2.2 Cells and reagents

The HepG2/C3A (CRL-10741) human hepatoma cell line was purchased from American Type Culture Collection, Manassas, VA. Minimum Essential Media (MEM), OptiMEM and fetal calf serum (FCS) were purchased from Life Technology, Melbourne, VIC, Australia. Small interfering RNA (siRNA) against *PEX13* and the non-specific control were purchased from Integrated DNA Technologies (IDT), Coralville, IA. The real-time PCR primer pairs (Supplementary Table 1) were also purchased from IDT. Antibodies used for Western blotting and immunofluorescence are listed in Supplementary Table 2.

2.3 Cell culture and gene knockdowns

HepG2/C3A cells were grown in a humidified atmosphere of 5% CO_2 at 37°C in MEM media supplemented with 10% FCS. For siRNA-mediated knock-down experiments, 6 X 10^5 cells were reverse transfected with 10pm non-specific control (siNS) and *PEX13*-specific siRNA (Supplementary Table 1) using Lipofectamine RNAiMAX (Life Technology), according to the manufacturer's recommendations. The knock-downs were carried out over a period of 72h, after which the cells were harvested for RNA isolation or Western blotting. The cells constitutively expressing HJV were generated previously in the laboratory and were maintained and cultured as per the conditions described previously [18].

2.4 Iron indices

Serum iron levels were determined using the commercial iron assay kit from PM Separations (Capalaba, QLD), as described previously [19]. Dry tissue iron concentrations were measured in the liver (HIC), spleen (SIC), heart (CIC), and duodenum (DIC), as previously described by Torrance and Bothwell [20].

2.5 Histology

Formalin (10%) fixed liver tissues were paraffin embedded, sectioned (3μM) and stained with hematoxylin and eosin (H&E) by Envoi Specialist Pathologists, Brisbane, QLD, Australia. To assess iron localization, sections were incubated in Perls' Prussian Blue staining solution, comprising equal parts of potassium ferrocyanide (Sigma-Aldrich, St. Louis, MO) and hydrochloric acid. Sections were then washed, counterstained with Nuclearfast Red (Sigma-Aldrich), dehydrated, cleared in xylene and mounted using Depex mounting medium. Liver sections were scanned using the

VS120 Olympus Slidescanner (Olympus Life Science Solutions, Waltham, MA) and imaged using OlyVIA software version 2.9 (Olympus Life Science Solutions).

2.6 Real-time PCR

Total RNA was extracted from mice tissues (liver, spleen and duodenum) or cells, using TRIsure™ (Bioline, Sydney, NSW, Australia) following the manufacturer's protocol. Total RNA (1µg) was reverse transcribed to cDNA using SensiFAST™ cDNA kit (Bioline). Real-time qPCR was performed using SensiFAST™ SYBR® No-Rox kit (Bioline) using primer pairs listed in Supplementary Table 1 on the QuantStudio™ 6 Flex Real-Time PCR System (Applied Biosystems™, Thermo Fisher Scientific, Seventeen Mile Rocks, QLD, Australia). The expression of all genes was normalized to the geometric mean of three reference genes: *β-actin*, hypoxanthine-guanine phosphoribosyl transferase (*HPRT*) and ribosomal protein L13 (*RPL13*) for cells, and *β-actin*, *Hprt* and DNA directed RNA polymerase II subunit RPB1 (*Polr2a*) for mice. The data was analyzed using ΔΔCT method as described previously [21].

2.7 Western blotting

Cell extracts were prepared in 1X sodium dodecyl sulphate (SDS) sample buffer and tissue homogenates from mice liver were prepared using Precellys tissue homogenizer (Bertin Instruments, Montigny-le-Bretonneux, France). Cell lysates (10µl) and tissue extracts (25µg) were electrophoresed on 10% or 12% SDS-polyacrylamide gels at 120V for 2h. The Trans-blot Turbo blotting apparatus (Bio-Rad Laboratories, Gladesville, NSW, Australia) was then used to transfer the proteins onto nitrocellulose membranes for 30min at 25V in transfer buffer (25mM TRIS, 192mM

glycine, 10% methanol). The membranes were blocked in 10% non-fat milk for 2h at room temperature and then incubated with primary antibodies (Supplementary Table 2) diluted in 10% non-fat milk at 4°C overnight. The membranes were then washed and incubated with HRP-conjugated secondary antibodies (Supplementary Table 2) in 10% non-fat milk for 2h at room temperature. The membranes were washed again and incubated with Lumina Forte Millipore chemiluminescent substrate (Millipore, Bayswater, VIC, Australia) for 5min at room temperature before being exposed to X-ray films for different exposure times. Films were developed using the Minolta film processor (Konica Minolta Medical and Graphic, Tokyo, Japan). ImageJ software (NIH, Bethesda, MD) was then used to perform densitometric analyzes to quantitate the proteins.

2.8 Immunofluorescence microscopy

Cells were seeded onto collagen-coated glass coverslips and reverse-transfected with siRNA (siNS or siPEX13) for 72h as described in section *2.3 Cell culture and gene knockdowns*. Cells were washed with PBSCM (1X PBS containing 1mM $CaCl_2$ and 1mM $MgCl_2$) and incubated with anti-Myc primary antibody (Supplementary Table 2) for 1h at room temperature. After washing the excess primary antibody off, the cells were fixed with cold 3% paraformaldehyde and incubated with secondary antibody, Alexa-fluor 488 (Supplementary Table 2) for 1h at room temperature, before washing and mounting them in Prolong Gold mounting media with DAPI (Thermo Fisher Scientific).

2.9 Flow cytometry analysis

Cells were washed in FACS buffer (2% FCS in PBS with 0.5mM EDTA) and incubated with primary antibody (see Supplementary Table 2) for 1h on ice in the dark. After repeated washes in FACS buffer, TFR1 expression was measured on the BD FACSCelesta (BD Biosciences, North Ryde, NSW, Australia) and analyzed with FlowJo software version 10 (Tree Star, Ashland, OR). For viability studies, cells were resuspended in propidium iodide (see Supplementary Table 2) diluted in FACS buffer and incubated for 15min at room temperature, prior to analysing on the flow cytometer.

2.10 Statistical analyses

Statistical analyses on variables between different groups were performed using student t-tests and one way ANNOVA. P values <0.05 were considered to be statistically significant. The GRAPHPAD PRISM 6 software (GraphPad Software, San Diego, CA) was used to perform the statistical analyses.

3. Results

3.1 Phenotypic characterization of the hepatocyte-specific Pex13 knock-out mouse model

Since total *Pex13* null mice show neonatal lethality [16], we generated mice with a hepatocyte-specific deletion of *Pex13*. The *Pex13* hepatocyte-specific knock-out mice (*Pex13$^{f/f}$/Alb-Cre$^{+/-}$*) presented with significantly less weight (Supplemental Figure 1) than their control littermates (*Pex13$^{f/f}$/Alb-Cre$^{-/-}$*), suggesting postnatal growth retardation as has been observed in patients [22] and mouse models [23] of peroxisomal disorders. However, we did not observe any differences in blood parameters except for neutrophils which were significantly lower in the *Pex13* hepatocyte-specific knock-out mice. The liver histology, as shown by H&E staining, showed no significant observable differences between the knock-out and control mice (Supplemental Figure 1). These results demonstrate the viability of mice with a hepatocyte-specific deletion of *Pex13*.

3.2 Iron parameters in the hepatocyte-specific Pex13 knock-out mouse model

To understand the consequences of abrogating *Pex13* expression in hepatocytes on systemic iron homeostasis, we measured tissue iron levels in the liver (HIC), spleen (SIC), heart (CIC) and duodenum (DIC) of 5-week old mice (Figure 1A). *Pex13$^{f/f}$/Alb-Cre$^{+/-}$* mice had a lower HIC compared to the *Pex13$^{f/f}$/Alb-Cre$^{-/-}$* mice, whereas the duodenum of the *Pex13$^{f/f}$/Alb-Cre$^{+/-}$* mice had significantly higher tissue iron levels. These results demonstrate a dysregulation in systemic iron homeostasis. Notably, there were no significant differences in total serum iron and transferrin saturation between the *Pex13$^{f/f}$/Alb-Cre$^{-/-}$* and *Pex13$^{f/f}$/Alb-Cre$^{+/-}$* mice (Figure 1A). Perls' staining

was also performed on the liver sections to examine the localization of iron in the livers. No morphological difference (Figure 1B) in iron localization was observed between the two groups.

3.3 Regulation of genes involved in iron homeostasis in the livers of the hepatocyte-specific Pex13 knock-out mouse model

We then examined the expression of genes involved in systemic regulation of iron homeostasis in the livers, spleen and duodenums of *Pex13$^{f/f}$/Alb-Cre$^{-/-}$* and *Pex13$^{f/f}$/Alb-Cre$^{+/-}$* mice. Real-time PCR analysis showed a significant decrease in the mRNA expression of *Pex13* in the livers of the *Pex13$^{f/f}$/Alb-Cre$^{+/-}$* mice (Figure 2A) but not in the spleen or duodenum (Supplemental Figure 2), consistent with the knock-out being hepatocyte-specific. We also measured the expression of proteins known to be involved in iron transport in the spleen and duodenums of these mice (Supplemental Figure 2). The *Pex13$^{f/f}$/Alb-Cre$^{+/-}$* mice have significantly lower divalent metal transporter 1 (*Dmt1*) (Supplemental Figure 2A) and transferrin receptor 1 (*Tfr1*) (Supplemental Figure 2B) expression in the spleen and duodenum respectively.

We measured the mRNA expression of transferrin receptors (*Tfr*), membrane-bound proteins involved in iron uptake and regulation in the livers of these mice. There was a significant reduction in the expression of *Tfr2* (Figure 2A) in the livers of *Pex13$^{f/f}$/Alb-Cre$^{+/-}$* mice. Next, we examined the expression of matriptase-2 (transmembrane serine protease 6) (*Tmprss6*) in the livers of both the *Pex13$^{f/f}$/Alb-Cre$^{-/-}$* and *Pex13$^{f/f}$/Alb-Cre$^{+/-}$* mice. Tmprss6 acts as a negative regulator of hepcidin. It cleaves hemojuvelin (Hjv) [24], which is a co-receptor for bone morphogenetic protein 6 (Bmp6) [25]. A significant decrease was observed in the mRNA expression levels of *Tmprss6* in the livers of

Pex13$^{f/f}$*/Alb-Cre*$^{+/-}$ mice (Figure 2A). These results suggest that the absence of *Pex13* in the liver may affect the expression of *Tfr2* and *Tmprss6*.

Hepcidin expression was also significantly lower in the livers of the *Pex13*$^{f/f}$*/Alb-Cre*$^{+/-}$ mice as compared to *Pex13*$^{f/f}$*/Alb-Cre*$^{-/-}$ mice (Figure 2B). Expression of *Bmp6*, an important mediator of hepcidin regulation in response to iron, did not change in the livers of the knock-out mice (Figure 2B). Inhibitor of DNA binding 1 (*Id1*) and *Smad7* are induced by the BMP-SMAD pathway and have been shown to be upregulated in hepcidin knock-out mice [26]. We observed a significant decrease in *Id1* mRNA levels (Figure 2B), however, *Smad7* expression was significantly increased in the livers of *Pex13*$^{f/f}$*/Alb-Cre*$^{+/-}$ mice compared to the *Pex13*$^{f/f}$*/Alb-Cre*$^{-/-}$ mice (Figure 2B).

We also examined the expression of signalling proteins involved in iron homeostasis in the livers of the *Pex13*$^{f/f}$*/Alb-Cre*$^{+/-}$ *mice* (Figure 3). There were no significant differences in phosphorylated Smad1/5/8 and fr1 levels in the livers of *Pex13*$^{f/f}$*/Alb-Cre*$^{-/-}$ and *Pex13*$^{f/f}$*/Alb-Cre*$^{+/-}$ mice. Similar to the mRNA levels, the Tfr2 protein levels were significantly reduced in the *Pex13*$^{f/f}$*/Alb-Cre*$^{+/-}$ mice, as compared to *Pex13*$^{f/f}$*/Alb-Cre*$^{-/-}$ mice. As expected there was a significant reduction in Pex13 protein levels in the livers of *Pex13*$^{f/f}$*/Alb-Cre*$^{+/-}$ mice as compared to their littermate controls.

3.4 Loss of PEX13 results in decreased hepcidin and increased *SMAD7 expression in HepG2/C3A cells*

To determine the molecular mechanisms of PEX13-mediated regulation of hepcidin, we targeted *PEX13* gene expression in HepG2/C3A using specific siRNA. In an initial screen of the hepatocyte cell lines generally used to examine molecular mechanisms

involved in iron homeostasis we identified C3A/HepG2 cell line as expressing the highest amounts of *PEX13* mRNA as compared to the others (Supplemental Figure 3A). Cell viability was not significantly affected by siRNA treatment (Supplemental Figure 3B). Real-time PCR analysis showed a significant knock-down (~10-fold) of the *PEX13* gene compared to the non-specific control siRNA (siNS) (Figure 4A). Western blotting demonstrated that PEX13 protein levels were also decreased following the 72h siRNA-mediated knock-down (Figure 4B). The siRNA-mediated loss of *PEX13* also resulted in a 3-fold decrease in the mRNA expression of hepcidin (*HEPC*) (Figure 4A).

We then examined the expression of molecules involved in BMP-SMAD signalling in these cells. We assessed the effect of *PEX13* knock-down on the expression of *ID1* and *SMAD7*. These factors have been previously reported to be upregulated in mouse liver in response to iron accumulation and are also regulated through the BMP-SMAD pathway [26]. *ID1* expression showed a similar trend to the mouse model where it was reduced in PEX13 knockdowns; an upregulation of *SMAD7* was observed in siPEX13 cells as compared to siNS (Figure 4A). These results suggest that a reduction in PEX13 expression may affect the expression of *SMAD7*.

3.5 PEX13 deficiency leads to increased endoplasmic reticulum stress

Endoplasmic reticulum (ER) stress is a known regulator of hepcidin; studies using cell and mouse models have shown that increased ER stress leads to a decrease in hepcidin synthesis [27, 28]. ER stress is also related to peroxisomal integrity and function; *Pex2*$^{-/-}$ mice showed an accumulation of the ER chaperone protein, glucose-regulated protein 78kDa (GRP78) [29], and a strong induction in the expression of ER

stress-related proteins in liver [30]. Similarly, an increase was observed in the expression of unfolded protein response (UPR) genes in *Pex5*-deficient hepatocytes [31]. These studies prompted us to examine the effect of loss of PEX13 on ER stress in HepG2/C3A cells.

A reduction in *PEX13* mRNA levels led to significant increases in the mRNA expression of cyclic AMP response element-binding protein H (*CREBH*) and endoplasmic reticulum degradation-enhancing alpha-mannosidase-like protein 3 (*EDEM3*), whereas the mRNA levels of the stress response protein, endoplasmic reticulum luminal protein (*ERp72)* were significantly lower in HepG2/C3A cells deficient in PEX13 (Figure 5. CREBH is a transcription factor which is known to be involved in the ER stress response. Previous studies have shown that treatment of cells with ER stress-inducing chemicals (tunicamycin) increased the expression of CREBH [32]. Similarly, EDEM3 is one of the chaperone proteins which are produced in the ER lumen and the mRNA expression of *EDEM3* is upregulated with an increase in ER stress [33]. These changes suggest that deficiency of PEX13 may result in ER stress leading to a downregulation of hepcidin expression.

We next examined the expression of these ER stress-related molecules in murine livers and as shown in Figure 6 A, there were significant increases in mRNA expression levels of C/EBP homologous protein (*Chop*), another transcription factor known to be activated by ER stress and *Edem3*, with a significant decrease in the expression of *Erp72*, suggesting an increase in ER stress as observed in the mouse model

3.6 TFR1 and HJV expression is decreased in HepG2/C3A cells upon loss of PEX13

In mRNA experiments, we observed a significant decrease in the levels of *Tfr2* and *Tmprss6* in the livers of *Pex13*$^{f/f}$*/Alb-Cre*$^{+/-}$ mice compared to *Pex13*$^{f/f}$*/Alb-Cre*$^{-/-}$ mice. Tfr2 and Tmprss6 are membrane proteins involved in the regulation of hepcidin. This suggested that loss of *Pex13* may affect the expression of some membrane proteins. We next examined whether the loss of PEX13 affects other components of the iron homeostasis machinery. We used siRNA-mediated knock-down of PEX13 in HepG2/C3A cells to study total and surface expression of endogenous TFR1 protein. Western blotting showed a decrease in total TFR1 protein levels in cells transfected with siPEX13 in comparison to those with siNS (Figure 7A). We also examined the surface expression of TFR1 in siNS and siPEX13 cells using flow cytometry and observed a significant decrease in TFR1-positive cells in the siPEX13 group as compared to siNS (Figure 7B).

Next we used HepG2/C3A cells constitutively expressing HJV [18] as a tool to study the effects of PEX13 knock-down on HJV. Immunofluorescence showed a significant decrease in the levels of cell surface HJV in siPEX13 cells (Figure 7C).

These results suggest that PEX13 may be important for maintaining the expression and function of membrane proteins involved in iron homeostasis.

4. Discussion

Peroxisomes are important cellular organelles required for both α and β-oxidation and synthesis of ether lipids. Peroxisomes also contain other enzymes with diverse functions such as oxidation (d-amino acid oxidases, 2-hydroxy acid oxidases (HAO), l-pipecolate oxidase); degradation of reactive oxygen species (catalase) and detoxification of glyoxylate (alanine glyoxylate aminotransferase) [11]. Peroxisomal disorders are characterized by pathologies in the central and peripheral nervous system but several other organs including the liver are also affected. Despite the known relationship between peroxisomal loss and hepatic dysfunction, it is unknown how the liver pathology in these disorders affects systemic iron homeostasis.

In the present study, we examined the relationship between PEX13, a peroxisomal membrane protein required for import of matrix proteins into peroxisomes and systemic iron homeostasis. Pups of *Pex13* mutant mice exhibit clinical features of Zellweger syndrome patients, including intrauterine growth retardation, severe hypotonia, failure to feed and neonatal death [16]. We generated mice with a hepatocyte-specific deletion of *Pex13* to examine the role of *Pex13* in liver iron homeostasis. Disruption of *Pex13* in mice resulted in a down-regulation of hepcidin gene expression. Similar results were obtained in HepG2/C3A cells using specific siRNA targeting *PEX13*. Our results indicate that loss of PEX13 causes disruptions in multiple molecules involved in hepcidin regulation and iron homeostasis.

The transgenic mice lacking hepatic *Pex13* expression had significantly reduced neutrophil counts. Previous studies have suggested an important role for peroxisomal lipid synthesis in neutrophil membrane stability. A decrease in peroxisome-derived membrane phospholipids increased ER stress and apoptosis in neutrophils [34]. Our

results suggest that loss of Pex13 function in the hepatocytes may result in a similar neutrophil phenotype.

Loss of PEX13 decreased hepcidin expression but increased *SMAD7* mRNA levels in both the livers of mice and HepG2/C3A cells. SMAD7 acts as an inhibitory SMAD by competing with receptor-activated SMADs for BMP receptors, thereby inhibiting the BMP-SMAD signalling and the subsequent expression of the target genes, including hepcidin [35]. Transgenic overexpression of *Smad7* in hepatocytes of mice has been shown to decrease hepcidin synthesis [36]. As we did not observe any changes in the phosphorylation of Smad1/5/8 in the livers of *Pex13*$^{f/f}$*/Alb-Cre*$^{+/-}$ mice compared to *Pex13*$^{f/f}$*/Alb-Cre*$^{-/-}$ mice, it is likely that the increase in *Smad7* expression is not affecting hepcidin expression through BMP-SMAD pathway.

We also found that deficiency of PEX13 can lead to a decrease in the expression of other proteins involved in iron homeostasis. *Pex13*$^{f/f}$*/Alb-Cre*$^{+/-}$ mouse liver exhibit significantly lower expression of *Tfr2*, a protein involved in the regulation of hepcidin. We and others have shown that loss of *Tfr2* in mice leads to reduced hepcidin levels in the liver [37-39]. We also observed a significant reduction in the surface expression of HJV, a known BMP-co-receptor [25]. Although both TFR2 and HJV play important roles in the BMP-SMAD- mediated hepcidin regulation, our results suggest that loss of *Pex13* may not affect phosphorylation of Smad1/5/8 in mice, hence the hepcidin dysregulation observed may be due to other molecular effects of Pex13. The reduction in the surface expression of both TFR1 and HJV is likely to be a consequence of membrane phospholipid deficiencies, that arise due to the biochemical abnormalities induced by peroxisomal deficiencies, caused in this case by the loss of PEX13. Plasmalogens are essential for proper membrane assembly and defects in

plasmalogen synthesis will lead to membrane instability and possibly improper localisation of membrane proteins as well.

Peroxins have been shown to play an important role in ER stress. *Pex2*$^{-/-}$ mice has significantly increased ER stress as indicated by an increase in the expression of ER stress markers [29, 30]. Similarly, *Pex5*$^{-/-}$ hepatocytes showed a significant increase in the expression of molecules involved in UPR [31]. Several studies have established the link between ER stress and systemic iron homeostasis. An increase in *CHOP* expression has been shown to lead to a suppression of hepcidin [27]. In this study, we were able to show that loss of *PEX13* in both mice livers and the HepG2/C3A hepatoma cell line leads to an increase in the expression of ER stress-related genes. These results suggest that a loss of *Pex13* expression and function can result in an increase in ER stress, which consequently plays a role in down-regulating the expression of hepcidin. These findings suggest other peroxisomal deficiencies leading to similar biochemical changes may also affect iron homeostasis proteins through increased ER stress, as has been observed in livers of other peroxisome deficiency mice models including Pex2 and Pex5 mutant mice [29-31].

Although we observed a significant reduction in mRNA levels of hepcidin in the livers of *Pex13*$^{f/f}$*/Alb-Cre*$^{+/-}$ mice, surprisingly this did not lead to an increase in either the HIC or serum iron levels. There was a significant increase in duodenal iron suggesting that iron is not being transported across the gut in the *Pex13*$^{f/f}$*/Alb-Cre*$^{+/-}$ mice. Additionally, there was a significant decrease in mRNA levels of *Tfr1* in the duodenum of *Pex13*$^{f/f}$*/Alb-Cre*$^{+/-}$ mice, suggesting an increase in iron levels. Taken together, these results suggest that loss of *Pex13* in hepatocytes may lead to a dysregulation in the expression of genes involved in maintaining systemic iron homeostasis.

Peroxisome biogenesis disorders are caused by mutations in the *PEX* genes, with some defects resulting in severe hypotonia, developmental defects, hepatic and renal abnormalities, and neonatal death. Defects in PEX13 lead to the Zellweger syndrome spectrum of disorders [10]. To date there has been only one case study that reported excessive body iron in two siblings suffering from Zellweger syndrome [12, 13]. Our study establishes a link between PEX13 and systemic iron homeostasis where a loss of Pex13 expression in the hepatocytes leads to a decrease in the expression of hepatic hepcidin and results in a decrease in the expression of membrane proteins (TFR1, TFR2 and HJV) on the surface of the cells. The ER stress and molecular changes caused by the deficiency of *Pex13* in the hepatocytes are similar to the changes observed in *Pex2* and *Pex5* mutant mice, suggesting that the hepatocyte defects and hepcidin dysregulation are more likely due to the biochemical abnormalities caused by defective peroxisomes in these models.

References

[1] J.J. Smith, J.D. Aitchison, Peroxisomes take shape, Nat Rev Mol Cell Biol, 14 (2013) 803-817.

[2] B. Distel, R. Erdmann, S.J. Gould, G. Blobel, D.I. Crane, J.M. Cregg, G. Dodt, Y. Fujiki, J.M. Goodman, W.W. Just, J.A. Kiel, W.H. Kunau, P.B. Lazarow, G.P. Mannaerts, H.W. Moser, T. Osumi, R.A. Rachubinski, A. Roscher, S. Subramani, H.F. Tabak, T. Tsukamoto, D. Valle, I. van der Klei, P.P. van Veldhoven, M. Veenhuis, A unified nomenclature for peroxisome biogenesis factors, J Cell Biol, 135 (1996) 1-3.

[3] T. Francisco, T.A. Rodrigues, A.F. Dias, A. Barros-Barbosa, D. Bicho, J.E. Azevedo, Protein transport into peroxisomes: Knowns and unknowns, Bioessays, 39 (2017).

[4] V. Dammai, S. Subramani, The human peroxisomal targeting signal receptor, Pex5p, is translocated into the peroxisomal matrix and recycled to the cytosol, Cell, 105 (2001) 187-196.

[5] S.J. Gould, J.E. Kalish, J.C. Morrell, J. Bjorkman, A.J. Urquhart, D.I. Crane, Pex13p is an SH3 protein of the peroxisome membrane and a docking factor for the predominantly cytoplasmic PTs1 receptor, J Cell Biol, 135 (1996) 85-95.

[6] H.R. Waterham, S. Ferdinandusse, R.J. Wanders, Human disorders of peroxisome metabolism and biogenesis, Biochim Biophys Acta, 1863 (2016) 922-933.

[7] A.M. Motley, P. Brites, L. Gerez, E. Hogenhout, J. Haasjes, R. Benne, H.F. Tabak, R.J. Wanders, H.R. Waterham, Mutational spectrum in the PEX7 gene and functional analysis of mutant alleles in 78 patients with rhizomelic chondrodysplasia punctata type 1, Am J Hum Genet, 70 (2002) 612-624.

[8] T. Baroy, J. Koster, P. Stromme, M.S. Ebberink, D. Misceo, S. Ferdinandusse, A. Holmgren, T. Hughes, E. Merckoll, J. Westvik, B. Woldseth, J. Walter, N. Wood, B. Tvedt, K. Stadskleiv, R.J. Wanders, H.R. Waterham, E. Frengen, A novel type of rhizomelic chondrodysplasia punctata, RCDP5, is caused by loss of the PEX5 long isoform, Hum Mol Genet, 24 (2015) 5845-5854.

[9] M.S. Ebberink, P.A. Mooijer, J. Gootjes, J. Koster, R.J. Wanders, H.R. Waterham, Genetic classification and mutational spectrum of more than 600 patients with a Zellweger syndrome spectrum disorder, Hum Mutat, 32 (2011) 59-69.

[10] Y. Liu, J. Bjorkman, A. Urquhart, R.J. Wanders, D.I. Crane, S.J. Gould, PEX13 is mutated in complementation group 13 of the peroxisome-biogenesis disorders, Am J Hum Genet, 65 (1999) 621-634.

[11] M. Baes, P.P. Van Veldhoven, Hepatic dysfunction in peroxisomal disorders, Biochim Biophys Acta, 1863 (2016) 956-970.

[12] J.M. Opitz, ZuRhein, G. M., Vitale, L., Shahidi, N. T., Howe, J. J., Chou, S. M., Shanklin, D. R., Sybers, H. D., Dood, A. R., and Gerritsen, T, The Zellweger syndrome (cerebro-hepato-renal syndrome), Birth Defects Orig. Art. Ser., 2 (1969) 144-160.

[13] L. Vitale, J.M. Opitz, N.T. Shahidi, Congenital and familial iron overload, N Engl J Med, 280 (1969) 642-645.

[14] J.N. Feder, A. Gnirke, W. Thomas, Z. Tsuchihashi, D.A. Ruddy, A. Basava, F. Dormishian, R. Domingo, Jr., M.C. Ellis, A. Fullan, L.M. Hinton, N.L. Jones, B.E.

Kimmel, G.S. Kronmal, P. Lauer, V.K. Lee, D.B. Loeb, F.A. Mapa, E. McClelland, N.C. Meyer, G.A. Mintier, N. Moeller, T. Moore, E. Morikang, C.E. Prass, L. Quintana, S.M. Starnes, R.C. Schatzman, K.J. Brunke, D.T. Drayna, N.J. Risch, B.R. Bacon, R.K. Wolff, A novel MHC class I-like gene is mutated in patients with hereditary haemochromatosis, Nat Genet, 13 (1996) 399-408.

[15] G. Rishi, D.F. Wallace, V.N. Subramaniam, Hepcidin: regulation of the master iron regulator, Biosci Rep, 35 (2015).

[16] M. Maxwell, J. Bjorkman, T. Nguyen, P. Sharp, J. Finnie, C. Paterson, I. Tonks, B.C. Paton, G.F. Kay, D.I. Crane, Pex13 inactivation in the mouse disrupts peroxisome biogenesis and leads to a Zellweger syndrome phenotype, Mol Cell Biol, 23 (2003) 5947-5957.

[17] S. Yakar, J.L. Liu, B. Stannard, A. Butler, D. Accili, B. Sauer, D. LeRoith, Normal growth and development in the absence of hepatic insulin-like growth factor I, Proc Natl Acad Sci U S A, 96 (1999) 7324-7329.

[18] C.J. McDonald, L. Ostini, N. Bennett, N. Subramaniam, J. Hooper, G. Velasco, D.F. Wallace, V.N. Subramaniam, Functional analysis of matriptase-2 mutations and domains: insights into the molecular basis of iron-refractory iron deficiency anemia, Am J Physiol Cell Physiol, 308 (2015) C539-547.

[19] G. Rishi, E.S. Secondes, D.F. Wallace, V.N. Subramaniam, Normal systemic iron homeostasis in mice with macrophage-specific deletion of transferrin receptor 2, Am J Physiol Gastrointest Liver Physiol, 310 (2016) G171-180.

[20] J.D. Torrance, T.H. Bothwell, A simple technique for measuring storage iron concentrations in formalinised liver samples, S Afr J Med Sci, 33 (1968) 9-11.

[21] C.J. McDonald, M.K. Jones, D.F. Wallace, L. Summerville, S. Nawaratna, V.N. Subramaniam, Increased iron stores correlate with worse disease outcomes in a mouse model of schistosomiasis infection, PLoS One, 5 (2010) e9594.

[22] S. Kumar, R. Suthar, S. Sharda, I. Panigrahi, R.K. Marwaha, Zellweger syndrome: prenatal and postnatal growth failure with epiphyseal stippling, Journal of pediatric endocrinology & metabolism : JPEM, 27 (2014) 185-188.

[23] S. Hiebler, T. Masuda, J.G. Hacia, A.B. Moser, P.L. Faust, A. Liu, N. Chowdhury, N. Huang, A. Lauer, J. Bennett, P.A. Watkins, D.J. Zack, N.E. Braverman, G.V. Raymond, S.J. Steinberg, The Pex1-G844D mouse: a model for mild human Zellweger spectrum disorder, Molecular genetics and metabolism, 111 (2014) 522-532.

[24] L. Silvestri, A. Pagani, A. Nai, I. De Domenico, J. Kaplan, C. Camaschella, The serine protease matriptase-2 (TMPRSS6) inhibits hepcidin activation by cleaving membrane hemojuvelin, Cell Metab, 8 (2008) 502-511.

[25] J.L. Babitt, F.W. Huang, D.M. Wrighting, Y. Xia, Y. Sidis, T.A. Samad, J.A. Campagna, R.T. Chung, A.L. Schneyer, C.J. Woolf, N.C. Andrews, H.Y. Lin, Bone morphogenetic protein signaling by hemojuvelin regulates hepcidin expression, Nat Genet, 38 (2006) 531-539.

[26] L. Kautz, D. Meynard, A. Monnier, V. Darnaud, R. Bouvet, R.H. Wang, C. Deng, S. Vaulont, J. Mosser, H. Coppin, M.P. Roth, Iron regulates phosphorylation of Smad1/5/8 and gene expression of Bmp6, Smad7, Id1, and Atoh8 in the mouse liver, Blood, 112 (2008) 1503-1509.

[27] S.J. Oliveira, J.P. Pinto, G. Picarote, V.M. Costa, F. Carvalho, M. Rangel, M. de Sousa, S.F. de Almeida, ER stress-inducible factor CHOP affects the expression of hepcidin by modulating C/EBPalpha activity, PLoS One, 4 (2009) e6618.

[28] C. Vecchi, G. Montosi, K. Zhang, I. Lamberti, S.A. Duncan, R.J. Kaufman, A. Pietrangelo, ER stress controls iron metabolism through induction of hepcidin, Science, 325 (2009) 877-880.

[29] W.J. Kovacs, K.N. Tape, J.E. Shackelford, T.M. Wikander, M.J. Richards, S.J. Fliesler, S.K. Krisans, P.L. Faust, Peroxisome deficiency causes a complex phenotype because of hepatic SREBP/Insig dysregulation associated with endoplasmic reticulum stress, J Biol Chem, 284 (2009) 7232-7245.

[30] W.J. Kovacs, K.N. Charles, K.M. Walter, J.E. Shackelford, T.M. Wikander, M.J. Richards, S.J. Fliesler, S.K. Krisans, P.L. Faust, Peroxisome deficiency-induced ER stress and SREBP-2 pathway activation in the liver of newborn PEX2 knock-out mice, Biochim Biophys Acta, 1821 (2012) 895-907.

[31] R. Dirkx, I. Vanhorebeek, K. Martens, A. Schad, M. Grabenbauer, D. Fahimi, P. Declercq, P.P. Van Veldhoven, M. Baes, Absence of peroxisomes in mouse hepatocytes causes mitochondrial and ER abnormalities, Hepatology, 41 (2005) 868-878.

[32] W.G. Jang, E.J. Kim, J.T. Koh, Tunicamycin negatively regulates BMP2-induced osteoblast differentiation through CREBH expression in MC3T3E1 cells, BMB Rep, 44 (2011) 735-740.

[33] K. Hirao, Y. Natsuka, T. Tamura, I. Wada, D. Morito, S. Natsuka, P. Romero, B. Sleno, L.O. Tremblay, A. Herscovics, K. Nagata, N. Hosokawa, EDEM3, a soluble EDEM homolog, enhances glycoprotein endoplasmic reticulum-associated degradation and mannose trimming, J Biol Chem, 281 (2006) 9650-9658.

[34] I.J. Lodhi, X. Wei, L. Yin, C. Feng, S. Adak, G. Abou-Ezzi, F.F. Hsu, D.C. Link, C.F. Semenkovich, Peroxisomal lipid synthesis regulates inflammation by sustaining neutrophil membrane phospholipid composition and viability, Cell Metab, 21 (2015) 51-64.

[35] S. Itoh, P. ten Dijke, Negative regulation of TGF-beta receptor/Smad signal transduction, Curr Opin Cell Biol, 19 (2007) 176-184.

[36] D. Lai, F. Teng, S. Hammad, J. Werle, T. Maas, A. Teufel, M.U. Muckenthaler, S. Dooley, M. Vujic Spasic, Hepatic Smad7 overexpression causes severe iron overload in mice, Blood, 131 (2018) 581-585.

[37] D.F. Wallace, L. Summerville, P.E. Lusby, V.N. Subramaniam, First phenotypic description of transferrin receptor 2 knockout mouse, and the role of hepcidin, Gut, 54 (2005) 980-986.

[38] D.F. Wallace, L. Summerville, V.N. Subramaniam, Targeted disruption of the hepatic transferrin receptor 2 gene in mice leads to iron overload, Gastroenterology, 132 (2007) 301-310.

[39] R.E. Fleming, J.R. Ahmann, M.C. Migas, A. Waheed, H.P. Koeffler, H. Kawabata, R.S. Britton, B.R. Bacon, W.S. Sly, Targeted mutagenesis of the murine transferrin receptor-2 gene produces hemochromatosis, Proc Natl Acad Sci U S A, 99 (2002) 10653-10658.

Figure Legends

Figure 1: Iron parameters in different tissues of hepatocyte-specific *Pex13* knock-out mouse model.

(A) Tissue iron concentrations in the liver (HIC: left top), spleen (SIC: right top), heart (CIC: left middle), duodenum (DIC: right middle), serum (left bottom) and transferrin saturation (right bottom) in the *Pex13$^{f/f}$/Alb-Cre$^{-/-}$* (n=5) and *Pex13$^{f/f}$/Alb-Cre$^{+/-}$* (n=6) mice. Results are presented as Mean±SEM and were analyzed by a student t-test (**=P<0.01, *=P<0.05).

(B) Perls' staining was performed on liver sections from representative 5-week old *Pex13$^{f/f}$/Alb-Cre$^{-/-}$* and *Pex13$^{f/f}$/Alb-Cre$^{+/-}$* mice.

Figure 2: Expression of genes involved in iron regulation in the hepatocyte-specific *Pex13* knock-out mouse model.

(A) Expression of genes known to be involved in iron-sensing was measured by RT-PCR. The relative mRNA expression of *Pex13* (left top), *Tfr1* (right top), *Tfr2* (left bottom) and *Tmprss6* (right bottom) in the livers of 5-week old *Pex13$^{f/f}$/Alb-Cre$^{-/-}$* (n=5) and *Pex13$^{f/f}$/Alb-Cre$^{+/-}$* (n=6) mice. Results are presented as Mean±SEM and were analyzed by a student t-test (**=P<0.01, *=P<0.05).

(B) RT-PCR was performed to measure the relative mRNA expression of genes involved in BMP-SMAD- mediated regulation of hepcidin. *Bmp6* (left top), hepcidin (*Hamp*) (right top), *Id1* (left bottom) and *Smad7* (right bottom) expression was measured in the livers of 5-week old *Pex13$^{f/f}$/Alb-Cre$^{-/-}$* (n=5) and *Pex13$^{f/f}$/Alb-Cre$^{+/-}$*

(n=6) mice. Results are presented as Mean±SEM and were analyzed by a student t-test (**=P<0.01, *=P<0.05).

Figure 3: Protein expression in livers of the hepatocyte-specific *Pex13* knock-out mouse model.

(A) To measure the protein expression levels of transferrin receptor 1 (Tfr1), Tfr2, Pex13 and phosphorylation of Smad1/5/8, Western blotting was performed on liver homogenates from 5-week old *Pex13*$^{f/f}$*/Alb-Cre*$^{-/-}$ (n=5) and *Pex13*$^{f/f}$*/Alb-Cre*$^{+/-}$ (n=6) mice. The image is a representative Western blot of Tfr1, Tfr2, total Smad1, phosphorylated Smad1/5/8 and Pex13.

(B) Protein levels of Tfr1 (left top), Tfr2 (right top), total Smad1 (left bottom) and phosphorylated Smad1/5/8 (right bottom) were quantified using ImageJ software. Results are presented as Mean±SEM, relative to *β*-actin and were analyzed by a student t-test (** = P<0.01).

Figure 4: Knock-down of PEX13 in HepG2/C3A cells leads to a dysregulation in hepcidin expression.

(A) RT-PCR was performed to measure the relative mRNA expression of *PEX13* (top left), *HEPC* (top right), *ID1* (bottom left) and *SMAD7* (bottom right) in HepG2/C3A cells, transfected with either 10pmol non-specific siRNA (siNS) or 10pmol PEX13-specifc siRNA (siPEX13) for 72h (n=3). Results are presented as Mean±SEM of three independent experiments performed in triplicate and analyzed by a student t-test (***=P<0.001, ****=P<0.0001).

(B) Western blotting was performed to measure the protein expression of PEX13 in HepG2/C3A cells transfected with either 10pmol non-specific siRNA (siNS) or 10pmol PEX13-specifc siRNA (siPEX13) for 72h. The image shows a representative Western blot of PEX13 in siNS and siPEX13 cells of three independent experiments performed in duplicate.

Figure 5: Loss of PEX13 in HepG2/C3A cells leads to increased ER stress.

RT-PCR was performed to measure the relative mRNA expression of *CREBH* (left top), *CHOP* (right top), *EDEM3* (left bottom) and *ERp72* (right bottom) in HepG2/C3A cells, transfected with either 10pmol non-specific siRNA (siNS) or 10pmol PEX13-specifc siRNA (siPEX13) for 72h (n=3). Results were analyzed by a student t-test. Three independent experiments were performed in triplicate (** = P<0.01).

Figure 6: *Pex13$^{f/f}$/Alb-Cre$^{+/-}$ mice* show an increase in the expression of ER stress genes in the livers.

RT-PCR was performed to measure the relative mRNA expression of *Crebh* (left top), *Chop* (right top), *Edem3* (left bottom) and *Erp72* (right bottom) in the livers of 5-week old *Pex13$^{f/f}$/Alb-Cre$^{-/-}$* (n=5) and *Pex13$^{f/f}$/Alb-Cre$^{+/-}$* (n=6) mice. Results are presented as Mean±SEM and were analyzed by a student t-test (** = P<0.01, * = P<0.05).

Figure 7: Expression of TFR1 and HJV is decreased upon loss of PEX13 in HepG2/C3A cells.

(A) Western blotting was performed to measure the protein expression of TFR1 in HepG2/C3A cells transfected with either 10pmol non-specific siRNA (siNS) or 10pmol PEX13-specifc siRNA (siPEX13) for 72h. The image is a representative Western blot of total TFR1 protein levels in siNS and siPEX13 cells. Three independent experiments were performed in duplicate.

(B) Surface expression of TFR1 was measured in HepG2/C3A cells transfected with either 10pmol non-specific siRNA (siNS) or 10pmol PEX13-specifc siRNA (siPEX13) for 72h using flow-cytometry. The image is a representative histogram for TFR1 surface expression in HepG2/C3A cells transfected with either siNS or siPEX13 (left). Frequency of TFR1 positive siNS and siPEX13 cells is also presented (right). Results are shown as Mean±SEM of three independent experiments performed in duplicate and analyzed by a student t-test (* = $P<0.05$).

(C) Immunofluorescence microscopy was performed to examine the surface expression of HJV in HepG2/C3A cells transfected with either 10pmol non-specific siRNA (siNS) or 10pmol PEX13-specifc siRNA (siPEX13) for 72h. The image shows immunofluorescent staining for surface expression of HJV (in green) in siNS and siPEX13-treated cells. Slides were imaged on Zeiss Z2 Axioimager microscope using a 63X oil objective. Scale bar is 20μm.

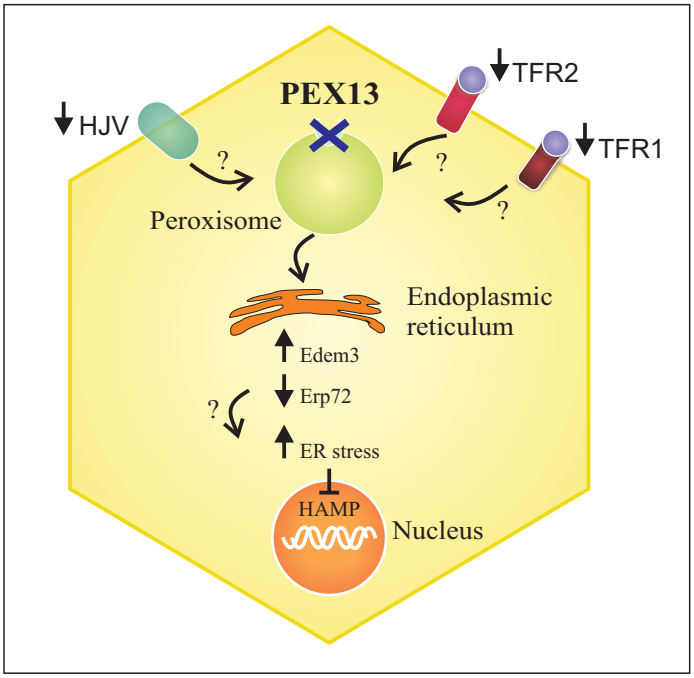
PEX13
TFR2
HJV
TFR1
?
?
?
Peroxisome
Endoplasmic
reticulum
Edem3
Erp72
?
ER stress
HAMP
Nucleus

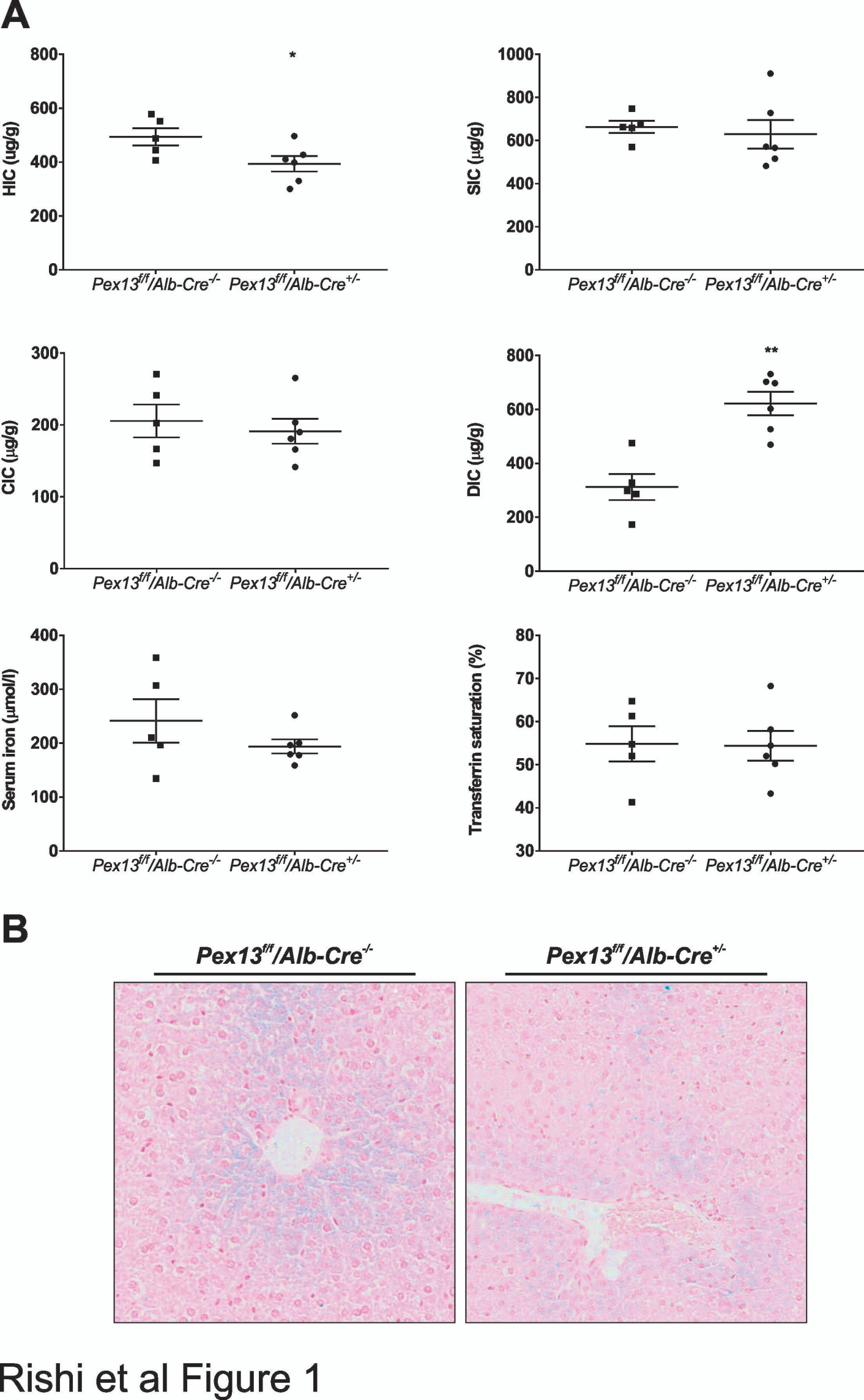

Rishi et al Figure 1

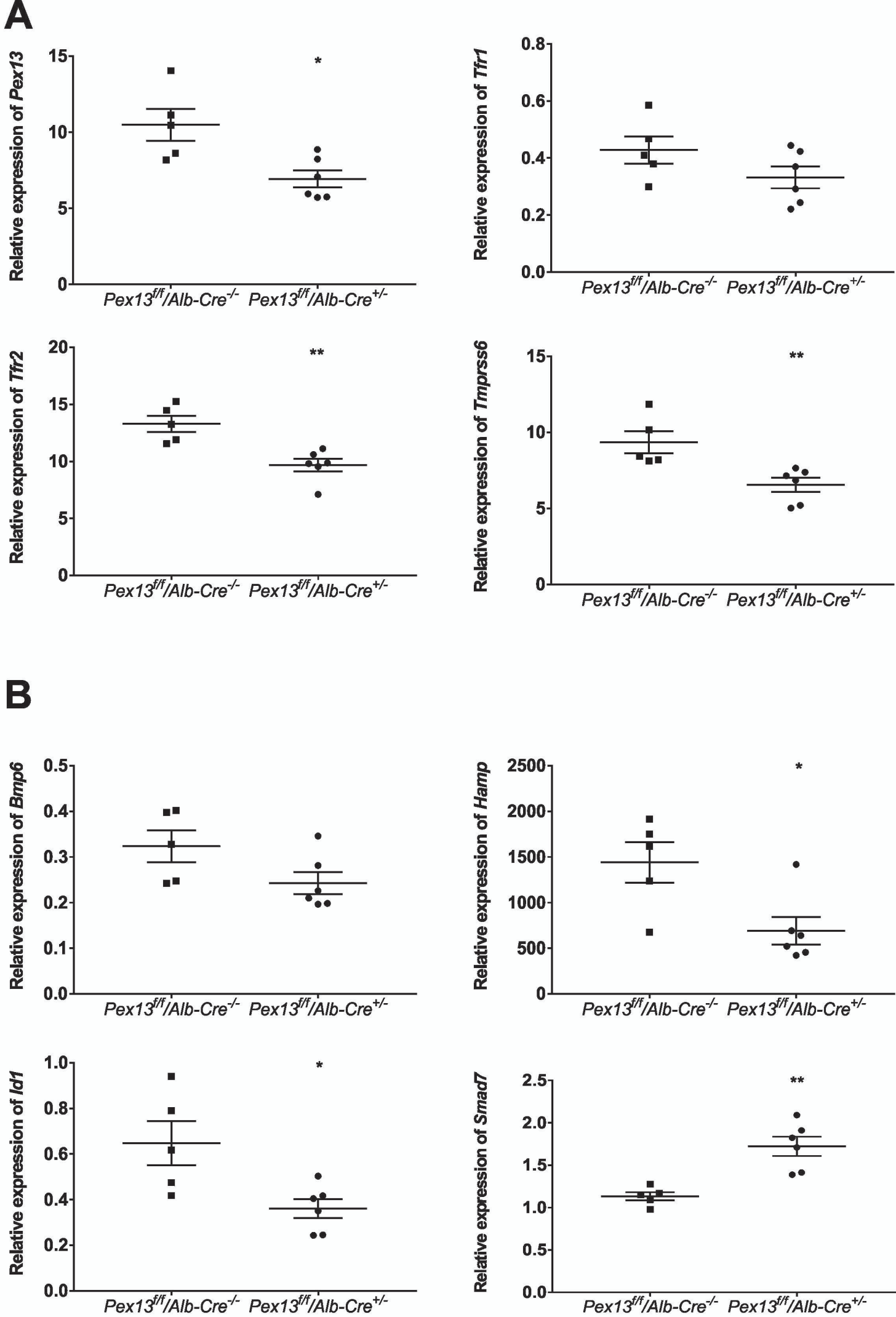

Rishi et al Figure 2

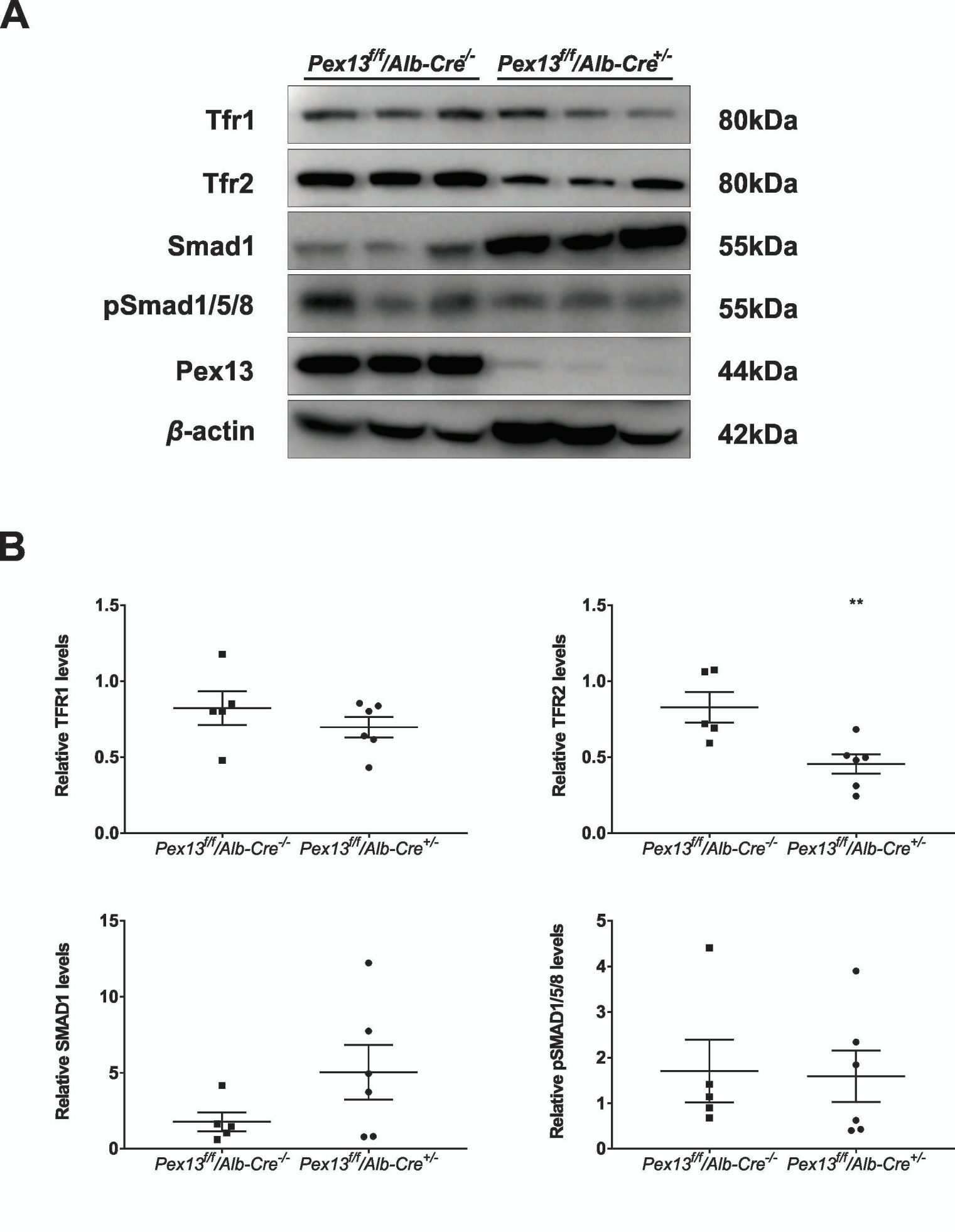

Rishi et al Figure 3

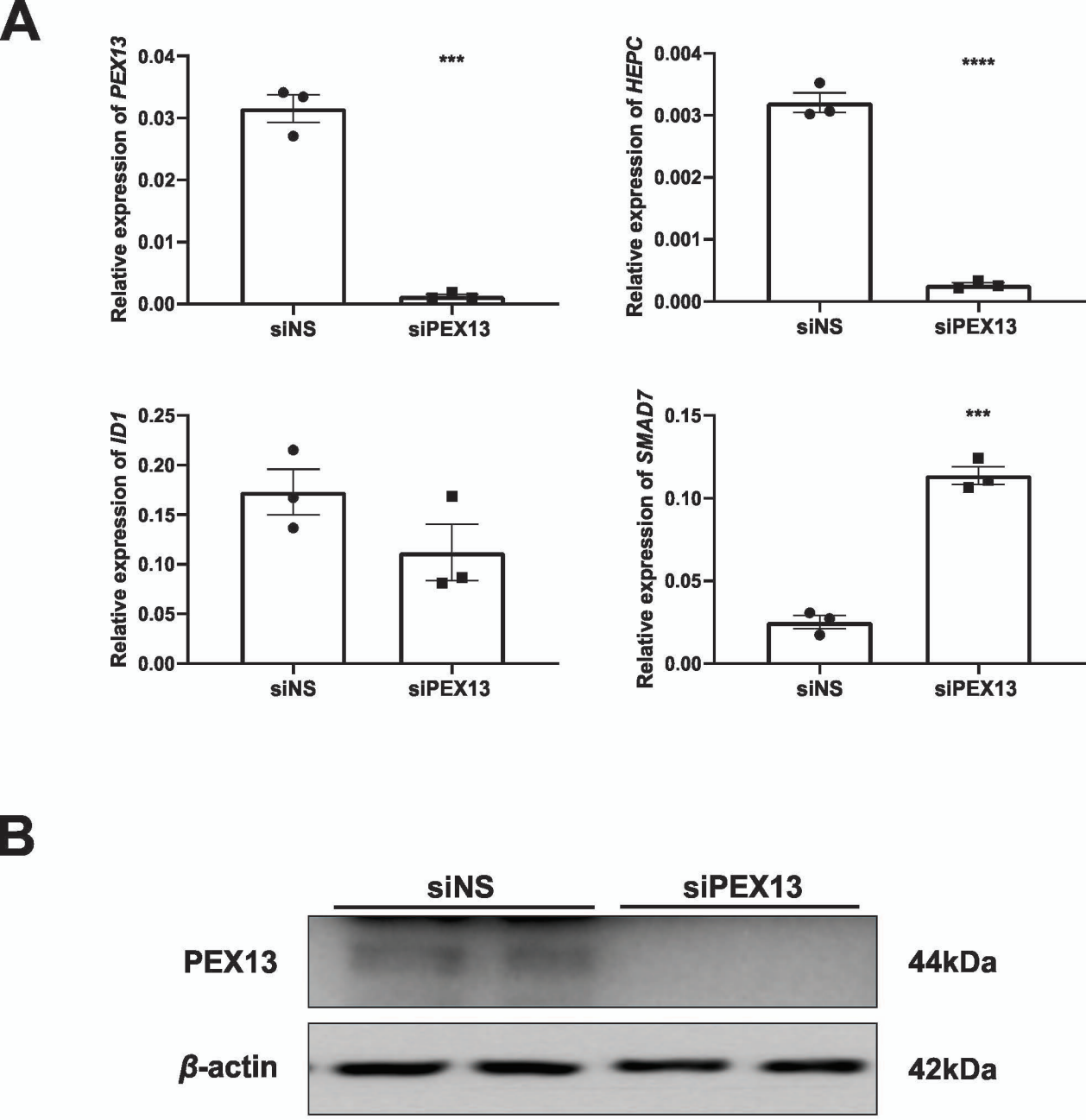

Rishi et al Figure 4

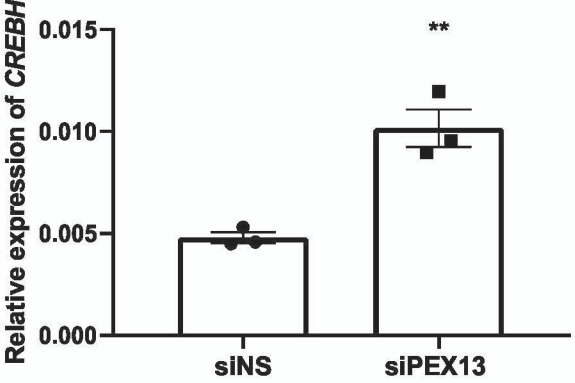

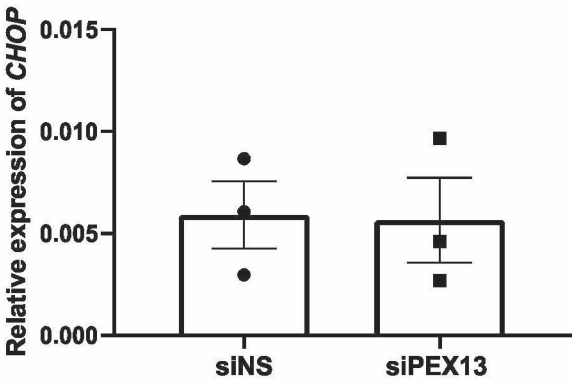

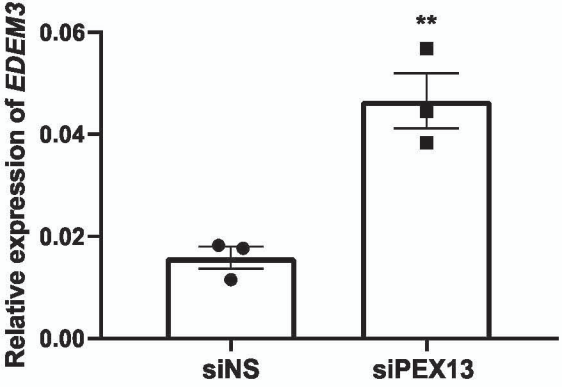

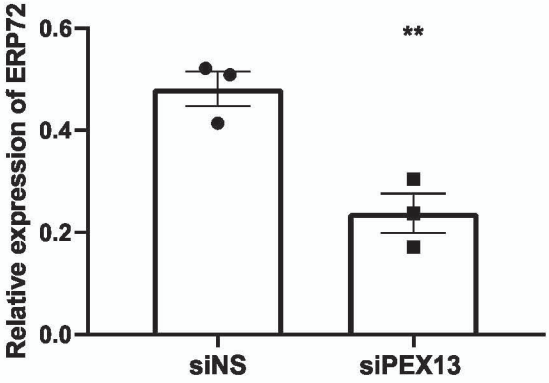

Rishi et al Figure 5

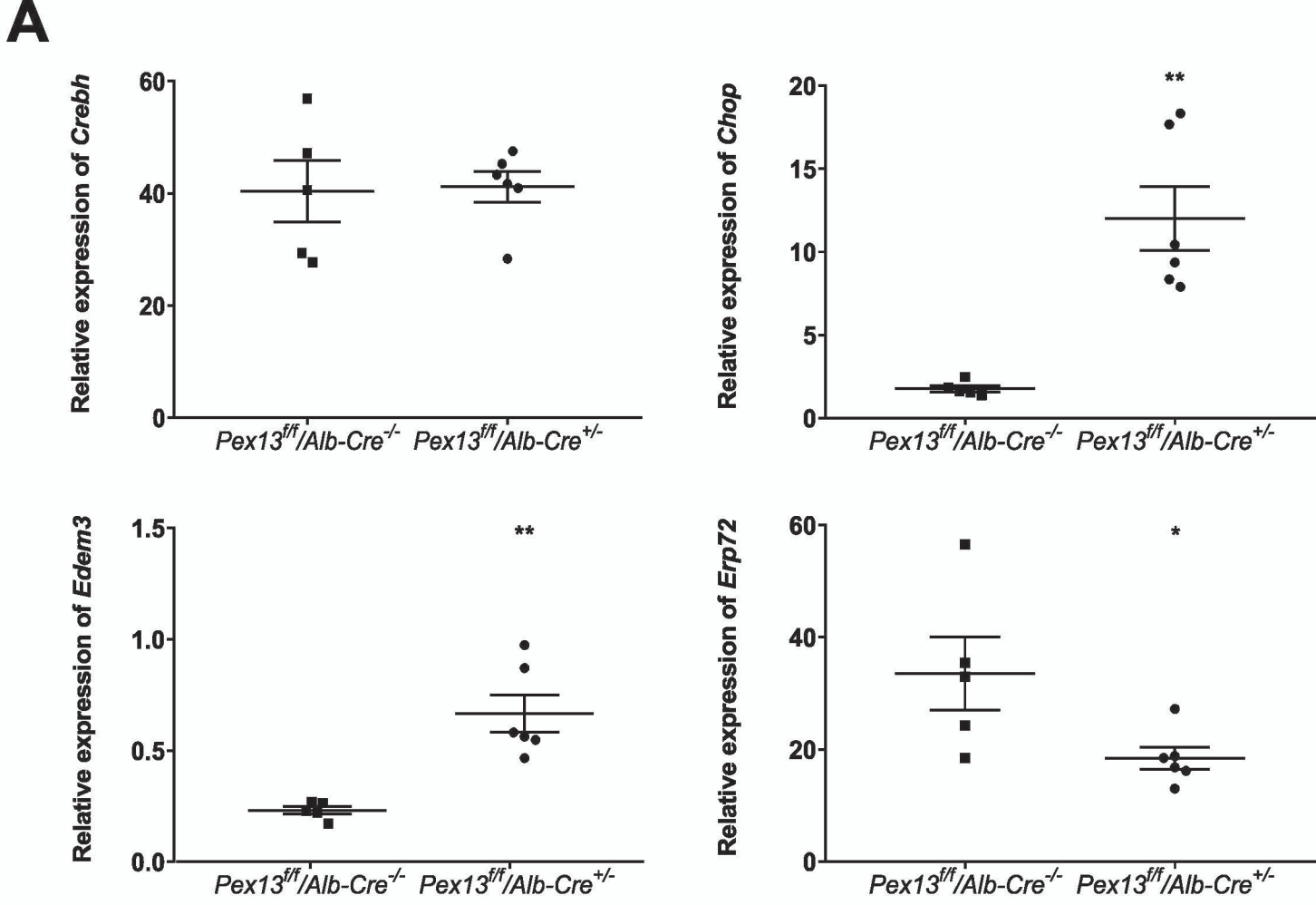

Rishi et al Figure 6

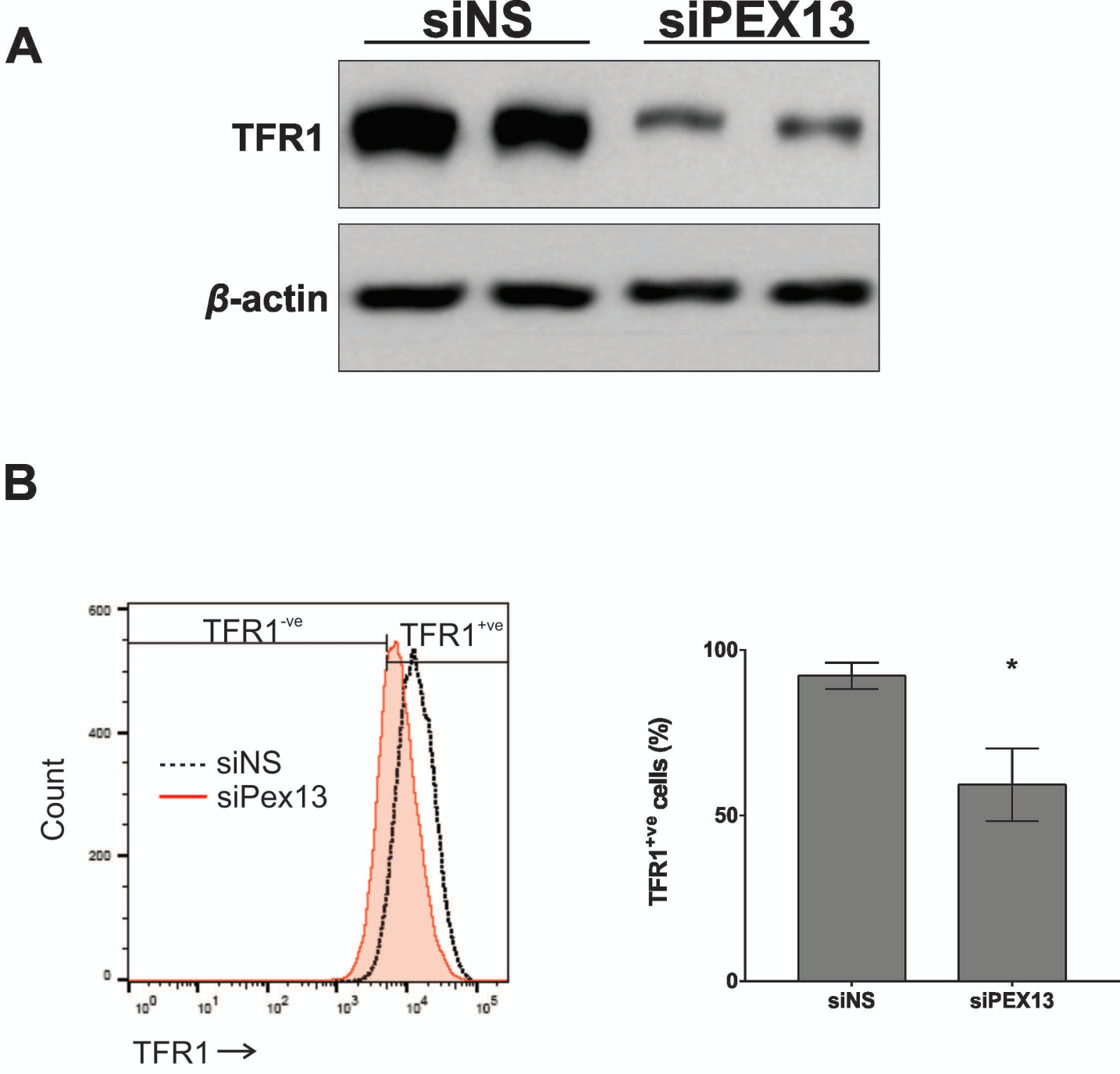

Rishi et al Figure 7

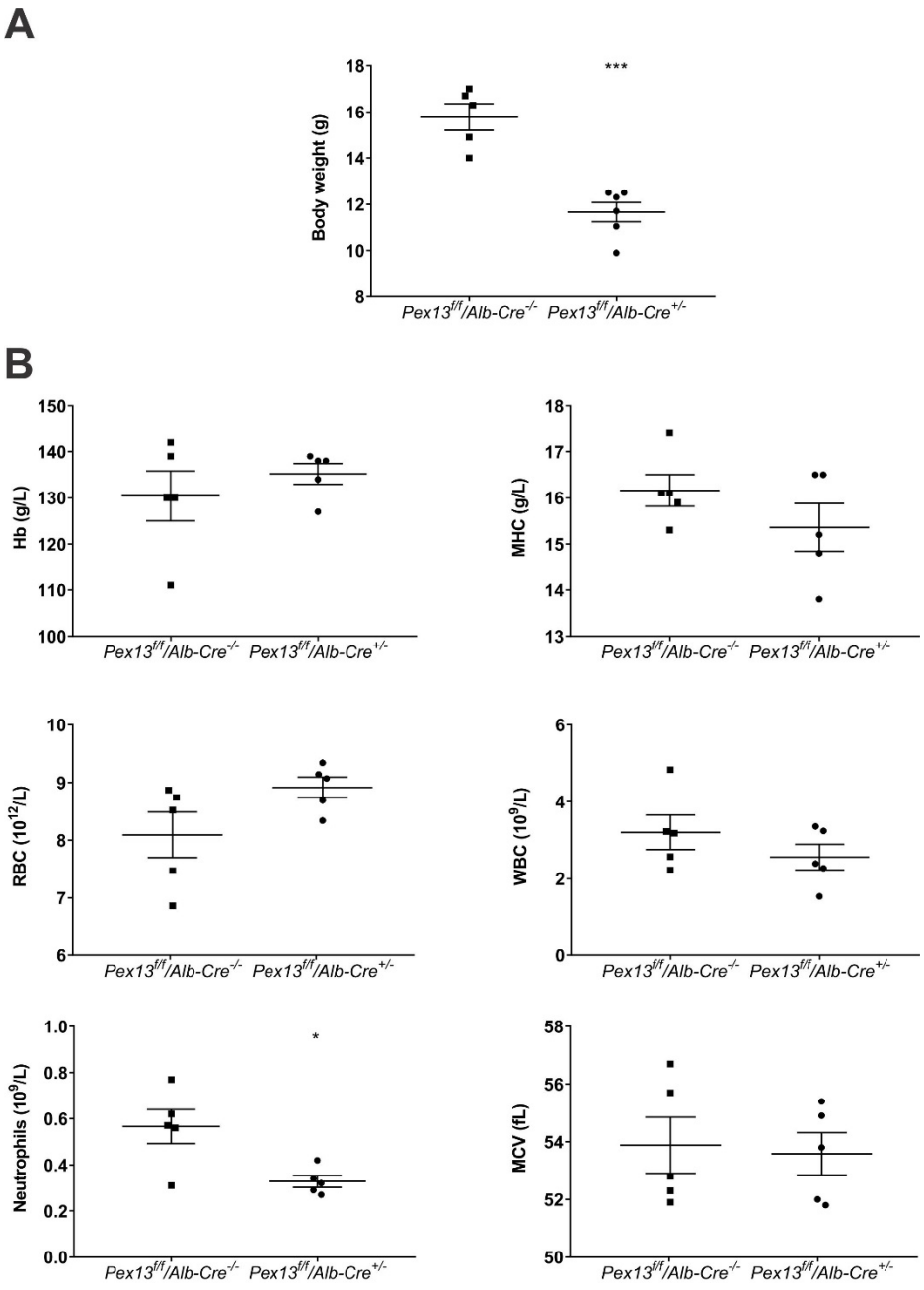

Rishi et al Figure S1

Figure S1: Phenotypic characterization of Pex13$^{f/f}$/Alb-Cre$^{+/-}$ mice.

Pex13$^{f/f}$/Alb-Cre$^{+/-}$ mice were characterized for (A) body weights , (B) blood indices and (C) histopathology.

(A) Body weights of 5-week old *Pex13$^{f/f}$/Alb-Cre$^{-/-}$*(n=5) and *Pex13$^{f/f}$/Alb-Cre$^{+/-}$* (n=6) mice. Results are presented as Mean±SEM and analyzed by a student t-test (***=P<0.001).

(B) Blood parameters, including hemoglobin (Hb) levels (left top), mean Hb concentration (MHC) (right top), red blood cell (RBC) count (left middle), white blood cell (WBC) count (right middle), neutrophil count (left bottom) and mean cell volume (MCV) (right bottom). Results are presented as Mean±SEM and analyzed by a student t-test (*= P<0.05).

(C) Histopathological analysis was performed on the liver sections of 5-week old *Pex13$^{f/f}$/Alb-Cre$^{-/-}$* and *Pex13$^{f/f}$/Alb-Cre$^{+/-}$* mice. The image is a representative H&E staining of liver sections.

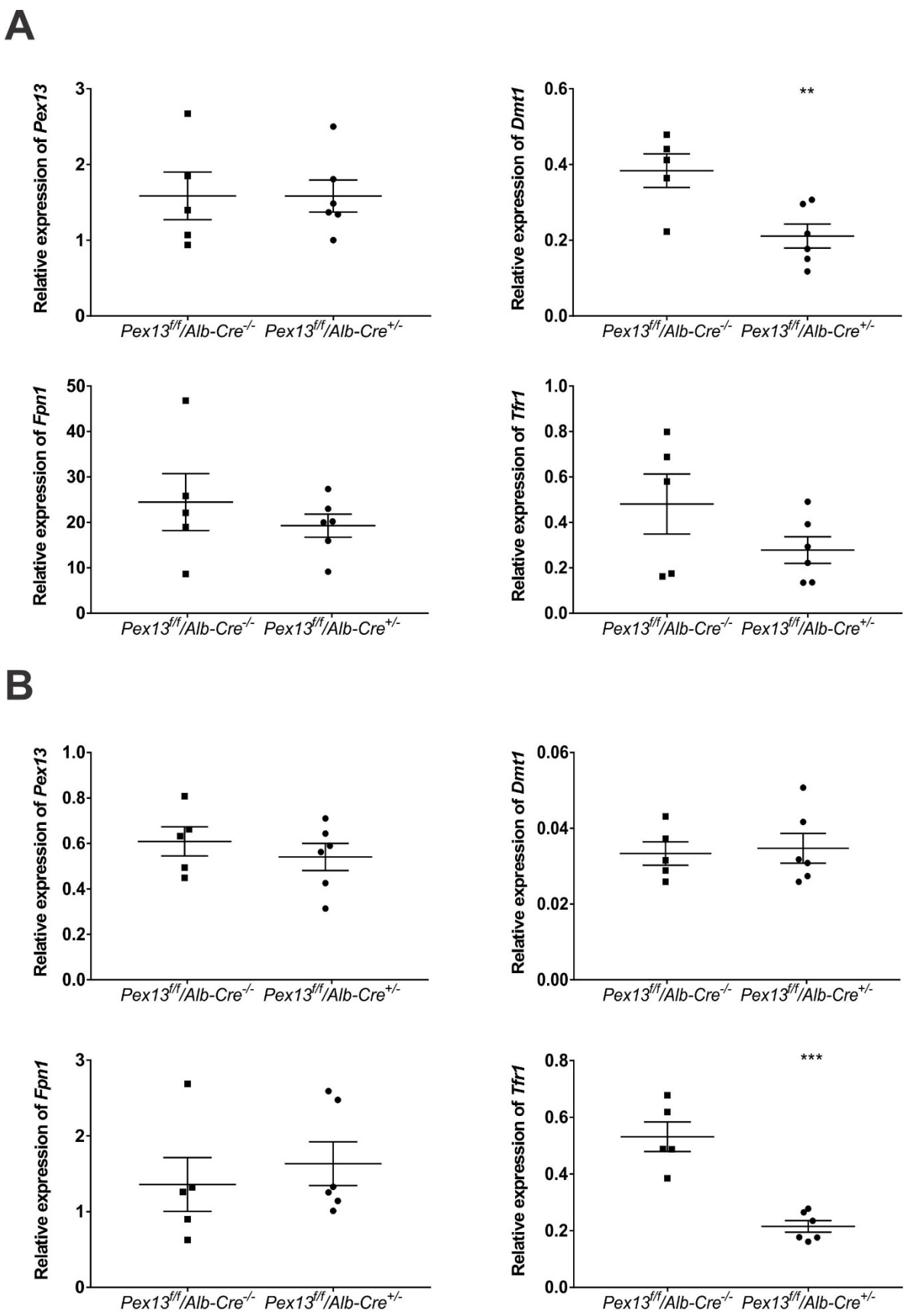

Rishi et al Figure S2

Figure S2: Expression of genes in the spleen and duodenum of the Pex13$^{f/f}$/Alb-Cre$^{-/-}$ and Pex13$^{f/f}$/Alb-Cre$^{+/-}$ mice.

RT-PCR was performed to measure the relative mRNA expression of *Pex13* (top left), *Dmt1* (top right), *Fpn1* (bottom left) and *Tfr1* (bottom right) in the (A) spleen of 5-week old *Pex13$^{f/f}$/Alb-Cre$^{-/-}$* (n=5) and *Pex13$^{f/f}$/Alb-Cre$^{+/-}$* (n=6) mice. Results are presented as Mean±SEM and were analyzed by a student t-test (** = P<0.01). (B) duodenum of 5-week old *Pex13$^{f/f}$/Alb-Cre$^{-/-}$* (n=5) and *Pex13$^{f/f}$/Alb-Cre$^{+/-}$* (n=6) mice. Results are presented as Mean±SEM and were analyzed by a student t-test (*** = P<0.001).

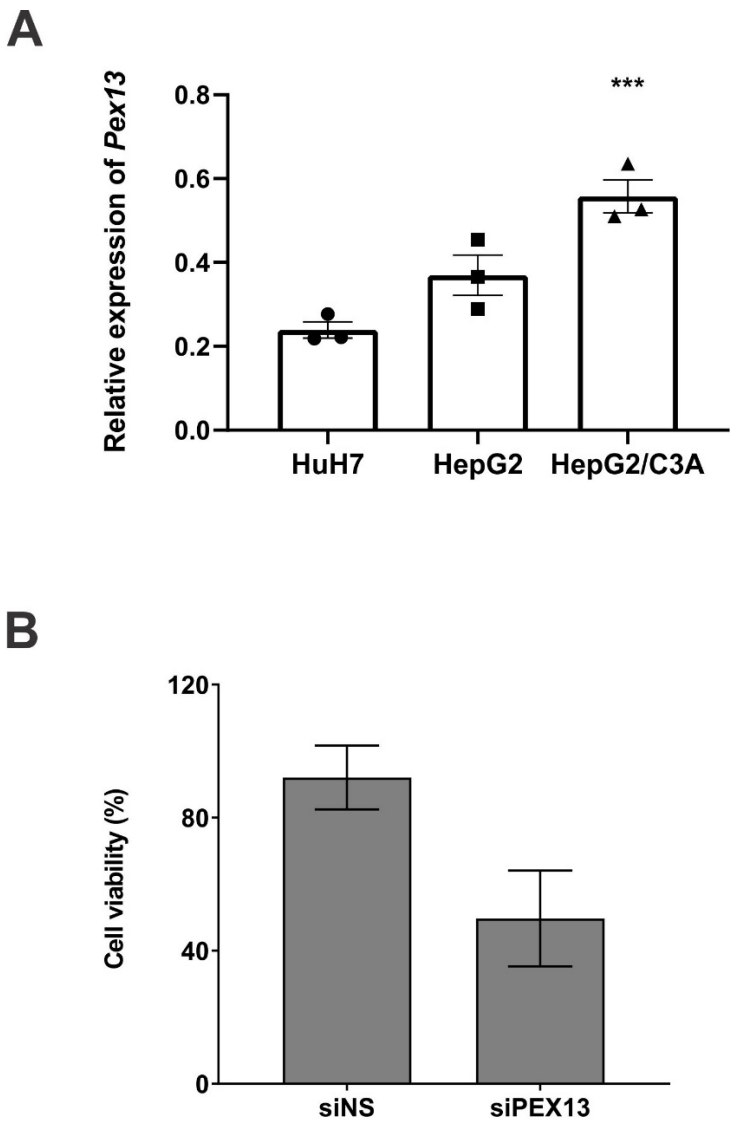

Rishi et al Figure S3

Figure S3: Viability of HepG2/C3A cells upon knock-down of PEX13.

(A) RT-PCR was performed to measure the relative mRNA expression of *PEX13* in HuH7, HepG2 and HepG2/C3A cells (n=3), Results are presented as Mean±SEM and were analyzed by one-way ANNOVA. (B) Viability of siNS and siPEX13 transfected cells was measured by propidium iodide staining and analyzed using flow cytometry. Results are presented as Mean±SEM and analyzed by a student t-test.

Supplementary Table 1: siRNA and real-time PCR primer pair sequences.

Primer	Sequence (5'3')
Mouse RT-PCR primers	
Actb-F	GACGGCCAAGTCATCACTATTG
Actb-R	CCACAGGATTCCATACCCAAGA
Hprt-F	GGACTGATTATGGACAGGA
Hprt-R	GAGGGCCACAATGTGATG
Polr2a-F	AGCTGGTCCTTCGAATCCGC
Polr2a-R	CTGATCTGCTCGATACCCTGC
Hamp-F	AGAGCTGCAGCCTTTGCAC
Hamp-R	ACACTGGGAATTGTTACAGCATTTA
Bmp6-F	ATGGCAGGACTGGATCATTG
Bmp6-R	CCATCACAGTAGTTGGCAGCG
TfR1-F	CATGAGGGAAATCAATGATCGTA
TfR1-R	GCCCCAGAAGATATGTCGGAA
Tfr2-F	CTATCTGGTCCTGATCACCCT
Tfr2-R	TCAGGGTTGACATCTTCATCGA
Fpn1-F	TTGCAGGAGTCATTGCTGCTA
Fpn1-R	TGGAGTTCTGCACACCATTGAT
Smad7-F	ACGGGAAGATCAACCCCGAG
Smad7-R	TTCCGCGGAGGAAGGTACAG
Dmt1-F	GGCTTTCTTATGAGCATTGCCTA
Dmt1-R	GGAGCACCCAGAGCAGCTTA
Pex13-F	GGCAAGTGGTGAGGATGACC
Pex13-R	CACGCACTTTGGGTTGTTGT

Id1-F	TCGTCGGTGGAACACATG
Id1-R	ACCCTGAACGGCGAGATCA
Tmprss6-F	CATCAACTTCACCTCCCAGA
Tmprss6-R	CAGTCCATTCACAGAGCAGAG
Crebh-F	CAGGCACTTGTGGTCCAGTCAA
Crebh-R	ACGAAGTCTCCAGGGCTGTCAA
Chop-F	GGAGGTCCTGTCCTCAGATGAA
Chop-R	GCTCCTCTGTCAGCCAAGCTAG
Edem3-F	CCACCACAAACCGAAGCATCTC
Edem3-R	GGTTCACGGATGCTCTGAGCAT
Erp72-F	TGGGCTCTTTCAGGGAGATGGT
Erp72-R	GGGAGACTTTCAGGAACTTGGC
Human RT-PCR primers	
β-ACTIN-F	CCGAGGACTTTGATTGCACATTG
β-ACTIN-R	TGGGGTGGCTTTTAGGATGG
HPRT-F	TTGCTTTCCTTGGTCAGGCA
HPRT-R	ATCCAACACTTCGTGGGGTC
RPL13-F	CCCCCAAGAAGGGAGACAGT
RPL13-R	GGAGACTAGCGAAGGCTTTGA
HAMP-F	CCACAACAGACGGGACAAC
HAMP-R	TCACCTTAGCCGACTCTGCG
SMAD7-F	TCACCTTAGCCGACTCTGCG
SMAD7-R	GTTTCAGCGGAGGAAGGCAC
ID1-F	TGGAGCTGAACTCGGAATCCG
ID1-F	GACACAAGATGCGATCGTCCG
CREBH-F	GAAGCCTCTGTGACCATAGACC

CREBH-R	GGAGGTCTTTCACGGTGAGATTG
CHOP-F	GGTATGAGGACCTGCAAGAGGT
CHOP-R	CTTGTGACCTCTGCTGGTTCTG
EDEM3-F	GCTTGGAGATGACAGTTTTCTGG
EDEM-R	CCATCCAAGTCCGAGCATTCAG
ERp72-F	CCAGCAGGTTTGATGTGAGTGG
ERp72-R	GGAGACTTCTCTGACCTTGGCA
PEX13-F	CCATGTAGTTGCCAGAGCAG
PEX13-R	CATCAAGGCTAGCCAGAAGC
siRNA sequences	
PEX13	CGGUGGAAUCAAGUAAAGUUUCCAA
	UUGGAAACUUUACUUGAUUCCACCGUU

Supplementary Table 2: Antibodies used in this study

Antibody	Use and dilution	Source
Anti-Pex13	Western blotting; 1 in 50,000	Gift from Prof Denis Crane, Griffith University, Australia (25)
β-actin	Western blotting; 1 in 20,000	Sigma
pSMAD1/5	Western blotting; 1 in 1000	Cell Signaling Technology (#9516)
SMAD1	Western blotting; 1 in 1000	Cell Signaling Technology (#9743)
TFR1	Western blotting; 1 in 1000	Zymed
TFR2	Western blotting; 1 in 10,000	(23)
Goat anti-Mouse HRP	Western blotting; 1 in 10,000	Thermo Fisher (#62-6520)
Goat anti-Rabbit HRP	Western blotting; 1 in 10,000	Thermo Fisher (#65-6120)
TFR1 surface (FITC anti-human CD71)	Flow cytometry; 1 in 250	BioLegend (#334103)
Propidium Iodide	Viability study; 1 in 500	Thermo Fisher (#P3566)
anti-Myc (71D10)	Immunofluorescence; 1 in 100	Cell Signaling Technology (#2278)
Alexa Fluor® 488 Donkey anti-Rabbit	Immunofluorescence; 1 in 100	Thermo Fisher (# A32790)